Formation Control of Underactuated Marine Vehicles with Communication Constraints

Even Børhaug, Alexey Pavlov, Reza Ghabcheloo, Kristin Y. Pettersen, António Pascoal, Carlos Silvestre.

***Abstract*— In this paper, we propose a nonlinear coordination control scheme for formation control of a group of underactuated marine vehicles with communication topology constraints. In particular, we propose decentralized control laws for coordinated path following of marine vehicles with sparse communication networks. The topology of the communication network is captured in the framework of graph theory and the proposed control scheme is applicable to communication networks with both bidirectional and unidirectional communication links.**

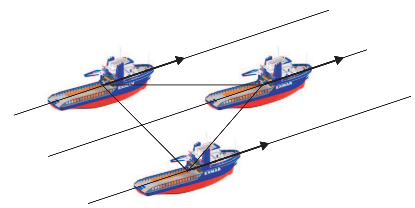

Fig. 1. Coordinated path following of three surface vessels.

I. INTRODUCTION

Formation control of marine vehicles is an enabling technology with a number of interesting applications. A fleet of multiple surface vessels moving together in a prescribed pattern can form an efficient data acquisition network for environmental monitoring and oil and gas exploration. Moreover, formation control techniques can be used to perform underway replenishment at sea, to perform automated towing operations of surface vessels, barges or oil platforms and to coordinate the motion between untethered underwater vehicles and surface vehicles in Long Baseline (LBL) communication configurations.

In this paper, we study coordinated formation control of a group of *underactuated* marine vehicles subject to communication topology constraints. In particular, we study coordinated path following of 3-DOF marine vehicles that are independently actuated in surge and yaw, but underactuated in sway. The marine vehicles can be surface vessels or underwater vehicles moving with constant depth. The objective is to control the vehicles at constant depth such that asymptotically they constitute a desired formation which then moves along a given path with a desired speed. This control objective can be achieved by, firstly, making each vehicle in the group follow a corresponding desired path and, secondly, by coordinating the motion of the vehicles along these paths such that they achieve the desired inter-vehicle spacing or formation pattern, as illustrated for the case of three vehicles in Figure 1.

While path following can be achieved by each individual vehicle independently of the others, the coordination of the vehicles requires inter-vehicle communication. The type of communication technology that can be used for inter-vehicle communication is greatly dependent on the application. For surface vessels, a communication network can be easily be established using radio transducers or optical transducers. However, both electromagnetic radio waves and light are heavily attenuated in water. For this reason, communication between underwater vehicles are typically achieved using acoustic modems. Acoustic communication is however plagued with errors, transmission delay, multi-path fading and directional limitations that greatly limit the range and bandwidth of the communication channels. Radio communication above the water surface is much more reliable and the bandwidth is much greater than underwater acoustic communication. However, transmitting the coordination information among all the vehicles can be time consuming, as only one vehicle can transmit on any given radio channel at a time. Also, loss of communication can occur due to failures or vessels moving out of range of each others radio. For this reasons, global information about all the vehicles in the group is generally not available to every vehicle. Instead of such a global exchange of information, inter-vehicle communication is given by the communication network topology that determines communication links between the vehicles. In this paper, the communication topology of the vehicles is captured in the framework of graph theory. Then, at the coordination stage, the constraints imposed by the topology of the inter-vehicle communication network are explicitly addressed. Furthermore, the controllability constraints resulting from the underactuation of the vehicles are addressed. To this end, we propose a nonlinear coordination control law that guarantees asymptotic coordination of the vehicles to the desired formation without violating the controllability constraints.

The problem of formation control with path following has been considered in a number of publications ([1], [2], [3], [4] and [5]). This problem is considered for *fully actuated* marine vehicles in [1] and [3]. Due to full actuation, there are no

E. Borhaug, A. Pavlov and K.Y. Pettersen are with the Dept. of Engineering Cybernetics, Norwegian University of Science and Technology, NO-7491 Trondheim, Norway. {E.Borhaug, Alexey.Pavlov, Kristin.Y.Pettersen}@itk.ntnu.no.

R. Ghabcheloo, A. Pascoal and C. Silvestre are with the Institute for Systems and Robotics and Dept. Electrical Engineering of IST, 1049-001 Lisbon, Portugal. {reza, antonio, cjs}@isr.ist.utl.pt

The work of R. Ghabcheloo, A. Pascoal and C. Silvestre was supported by project MAYA-Sub of the AdI and the FCT (ISR/IST plurianual funding) - through the POS Conhecimento Program that includes FEDER funds. R. Ghabcheloo benefited from an FCT scholarship while visiting the NTNU.

controllability constraints that have to be taken into account and, therefore, coordination can be achieved by standard linear control laws. Apart from [3], which also allows for communication networks with directed communication links, communication topologies studied in these papers allow for only bidirectional communication links between the vehicles. For underactuated systems, formation control with path following has been considered in [2] and [4]. The result of [2] is essentially limited to vehicles in a leader-follower configuration, while [4] allows for more general configurations. While the necessity of the controllability constraints has been formulated in these papers, the coordination control laws proposed in these works do not take into account these constraints. The controllability constraints have been explicitly taken into account in [5]. Yet, in this paper only the case of bidirectional inter-vehicle communications has been considered.

Therefore, the main contribution of this paper is the design of controllers for formation control with path following with a nonlinear coordination control law that takes into account the controllability constraints arising due to underactuation and that is suitable for sparse communication networks with both unidirectional and bidirectional communication links.

II. Vehicle Model and Control Objective

In this section we present the kinematic and dynamic model describing the motion of the class of marine vehicles studied in this paper. Moreover, we define the notation used throughout the paper and state the control problem to be solved.

A. Single Vehicle Model

We consider an underactuated marine vehicle described by the 3-DOF model [6]:

$$\dot{x} = u\cos\psi - v\sin\psi \tag{1}$$

$$\dot{y} = u\sin\psi + v\cos\psi \tag{2}$$

$$\dot{\psi} = r \tag{3}$$

$$\boldsymbol{M}\dot{\boldsymbol{\nu}} + \boldsymbol{C}(\boldsymbol{\nu})\boldsymbol{\nu} + \boldsymbol{D}\boldsymbol{\nu} = \boldsymbol{B}\boldsymbol{u}, \tag{4}$$

where $\boldsymbol{\nu} \triangleq [u, v, r]^T$. Here, u and v are the surge and sway velocity respectively, and r is the yaw rate. Moreover, (x, y) is the inertial position of the vehicle and ψ is the yaw angle. The matrix $\boldsymbol{M} = \boldsymbol{M}^T > 0$ is the mass and inertia matrix, $\boldsymbol{C}(\boldsymbol{\nu})$ is the Coriolis and centripetal matrix and $\boldsymbol{D} > 0$ is the damping matrix and they are given by ([6]):

$$\boldsymbol{M} = \begin{bmatrix} m_{11} & 0 & 0 \\ 0 & m_{22} & m_{23} \\ 0 & m_{23} & m_{33} \end{bmatrix}, \boldsymbol{D} = \begin{bmatrix} d_{11} & 0 & 0 \\ 0 & d_{22} & d_{23} \\ 0 & d_{32} & d_{33} \end{bmatrix},$$

$$\boldsymbol{C}(\boldsymbol{\nu}) = \begin{bmatrix} 0 & 0 & -m_{22}v - m_{23}r \\ 0 & 0 & m_{11}u \\ m_{22}v + m_{23}r & -m_{11}u & 0 \end{bmatrix}.$$

The vector $\boldsymbol{u} \triangleq [T_u, T_r]^T$ is the control input, where T_u is the surge thrust and T_r is the yaw torque respectively, and the matrix $\boldsymbol{B}$ is a 3×2 actuator configuration matrix with full column rank. Note that the class of vehicles considered in this paper is underactuated, as only 2 independent controls are available to control 3 degrees of freedom. Moreover, we assume that the control input does not affect the sway motion, in the sense that $\boldsymbol{M}^{-1}\boldsymbol{B}\boldsymbol{u} \triangleq [\tau_u, 0, \tau_r]^T$. Note that for a large class of marine vehicles, the body-fixed coordinate system can be chosen such that the control input does not affect the sway motion (see e.g. [7]).

In Section III, we will derive a surge controller that guarantees that $|u(t)| \le U_{\max}$, $\forall t \ge t_0$, where $U_{\max} > 0$ is the largest permissible surge speed. To aid the analysis of the remaining dynamics, we make the following assumptions:

$$|v| \le C_v U_{\max}|r|, \tag{5}$$

$$|v| \le U_{\max}, \tag{6}$$

for some constant $C_v > 0$. These assumptions can be justified for most underactuated surface vessels since the hydrodynamic damping in the sway direction is usually much larger compared to the surge direction. Therefore, the forward velocity (satisfying $|u| \le U_{\max}$) becomes dominant, see (6). Assumption (5) means that if the angular rate r converges to zero, the sway velocity v is damped out and also converges to zero. This is a natural assumption for most marine vehicles, since the sway motion is heavily damped due to hydrodynamic drag and since the control input does not affect the sway motion. Also, the Munk moment, the destabilizing moment that tries to turn the vehicle, is zero for $r = 0$.

B. Control Objective

In this paper, we deal with formation control of underactuated marine vehicles. We will design decentralized control laws for n vehicles such that after transients the vehicles form a desired formation and move along a desired straight-line path $\boldsymbol{L}$ with a given velocity profile $u_d(t)$, as illustrated in Fig. 2. The main focus of the paper is the design of a nonlinear decentralized *coordination control law* for a group of n vehicles with restricted inter-vehicle communication. In this section we define the control problem and formalize the problem to be solved.

Consider a group of n vehicles described by the model (1)-(4) and satisfying assumptions (5), (6), together with a given desired formation pattern, a straight-line path $\boldsymbol{L}$ to be followed by the formation and a desired formation velocity profile $u_d(t)$. The formation control objective is then to design feedback controllers for each vehicle in the group such that, after transients, the vehicles satisfy the desired formation pattern and the formation moves synchronously along $\boldsymbol{L}$ with velocity profile $u_d(t)$. In this paper, we view the formation control problem as a coordinated path following problem. That is, given $\boldsymbol{L}$ and a desired formation pattern, we define n translated paths $\boldsymbol{L}_j$, $j = 1, \ldots, n$. The formation control objective can then be achieved in two steps. The first step is to make vehicle j follow path $\boldsymbol{L}_j$ with a commanded velocity. The second step is to coordinate the motion of the vehicles by controlling the commanded velocity of the vehicles so that they form the desired formation pattern and move synchronously with the desired velocity profile $u_d(t)$.

We choose the inertial coordinate system with the x-axis along the desired path of the formation, with the z-axis pointing down, and denote the position of vehicle j, in the chosen inertial coordinate system, by (x_j, y_j). The formation is characterized by a formation reference point $\boldsymbol{r}(t)$ and a set of vectors $\boldsymbol{r}_j \triangleq [D_{x_j}, D_{y_j}]^T$, $j = 1, \ldots, n$, giving the desired position of vehicle j with respect to the reference point (see Fig. 2). Moreover, with this particular choice of the inertial coordinate system, the desired path for vehicle j is $\boldsymbol{L}_j = \{(x, y) \in \mathbb{R}^2 \mid y - D_{y_j} = 0\}$. With this notation,

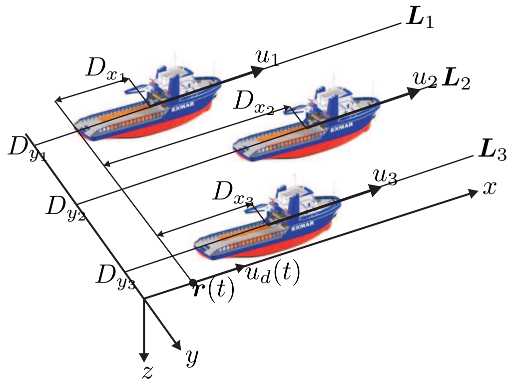

Fig. 2. Illustration of formation.

the control objective can be formalized as follows:

$$\lim_{t \to +\infty} y_j(t) - D_{y_j} = 0, \quad j = 1, \ldots, n, \tag{7}$$

$$\lim_{t \to +\infty} \psi_j(t) = 0, \quad j = 1, \ldots, n, \tag{8}$$

$$\lim_{t \to +\infty} x_1(t) - D_{x_j} = \ldots = x_n(t) - D_{x_n}, \tag{9a}$$

$$\lim_{t \to +\infty} \dot{x}_j(t) = u_d(t), \quad j = 1, \ldots, n. \tag{9b}$$

The above stated control problem will be solved in two stages. In the first stage, we will design independent path following controllers for each vehicle in the group so that control goals (7), (8) are achieved. Moreover, we will design controllers for each vehicle such that the vehicles track commanded velocity profiles $u_{c_j}(t)$, which will be specified at a later stage. Thus, in the first stage, we also have the auxiliary control objective

$$\lim_{t \to +\infty} u_j(t) - u_{c_j}(t) = 0, \quad j = 1, \ldots, n. \tag{10}$$

This part of controller design is presented in Section III. In the second stage, we develop controllers for u_{c_j} that coordinate the motion of the vehicles along the desired paths such that the vehicles achieve the desired formation pattern and move synchronously with desired velocity profile $u_d(t)$, as specified in the coordination control goal (9). These controllers are presented in Section IV.

III. Path Following Control

To satisfy the control goal (10) and make each vehicle exponentially track its commanded velocity profile $u_{c_j}(t)$, we propose the following feedback linearizing control law for τ_{u_j} :

$$\tau_{u_j} = -1/m_{11}(m_{22}v_j + m_{23}r_j)r_j + \dot{u}_{c_j} - k_{u_j}(u_j - u_{c_j}), \tag{11}$$

where $k_{u_j} > 0$. To satisfy the control goals (7), (8), we make ψ_j, $j = 1, \ldots, n$, track a Line of Sight (LOS) angle:

$$\psi_{\mathrm{LOS},j} = -\tan^{-1}\left(\frac{y_j - D_{y_j}}{\Delta}\right), \quad j = 1, \ldots, n, \tag{12}$$

where $\Delta > 0$, is the look-ahead distance. See Figure 3 for a geometrical interpretation of the LOS angle $\psi_{\mathrm{LOS},j}$. To make

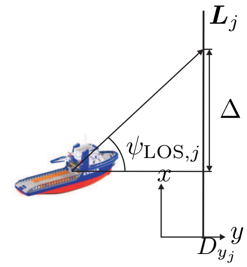

Fig. 3. Illustration of the LOS angle $\psi_{\mathrm{LOS},j}$.

ψ_j exponentially track $\psi_{\mathrm{LOS},j}$, $j = 1, \ldots, n$, we propose the following feedback linearizing control law for τ_{r_j}:

$$\begin{aligned}\tau_{r_j} = &-\frac{m_{22}}{\Lambda}[(-m_{22}v_j - m_{23}r_j)u + m_{11}u_j v_j \\ &- d_{32}v_j - d_{33}r_j] + \frac{m_{23}}{\Lambda}(-m_{11}u_j r_j - d_{22}v_j - d_{23}r_j) \\ &+ \dot{r}_{d_j} - k_{r_j}(r_j - r_{d_j}),\end{aligned} \tag{13}$$

where $\Lambda = m_{22}m_{33} - m_{23}^2 > 0$, $k_{r_j} > 0$ and r_{d_j} is given by the expression

$$r_{d_j} = \frac{\Delta}{e_j^2 + \Delta^2}(u_j \sin\psi_j + v_j \cos\psi_j) - k_{\psi_j}(\psi_j - \psi_{\mathrm{LOS},j}), \tag{14}$$

where $k_{\psi_j} > 0$. We then have the following result:

Proposition 1 (Path following)**.** *Consider a marine vehicle described by the model (1)-(4) and satisfying assumptions (5) and (6). If $u_{c_j}(t) \in (U_{\min}, U_{\max})$, $\forall t \geq t_0$, where $\Delta > U_{\max}C_v$ and $U_{\min} > 0$, then the surge controller (11) and the yaw controller (13) guarantee that the control goals (7), (8) and (10) are achieved exponentially.*

Proof. Define $\tilde{u}_j \triangleq u_j - u_{c_j}(t)$. The feedback control law (11) linearizes the surge dynamics and makes the origin of the closed loop surge tracking error dynamics uniformly globally exponentially stable (UGES):

$$\dot{\tilde{u}}_j = -(k_{u_j} + d_{11})\tilde{u}_j, \tag{15}$$

where $d_{11} > 0$, since $\boldsymbol{D} > 0$. Hence, the controller (11) guarantees that for all initial conditions $\tilde{u}_j(t_0) \in \mathbb{R}$, $t_0 \in \mathbb{R}^+$, the control goal (10) is achieved exponentially.

Define $\tilde{\psi}_j \triangleq \psi_j - \psi_{\mathrm{LOS},j}$ and $\tilde{r}_j \triangleq r_j - r_{d_j}$. The feedback control law (13) linearizes the yaw rate dynamics and makes the yaw angle and yaw rate error dynamics UGES:

$$\dot{\tilde{\psi}}_j = -k_{\psi_j}\tilde{\psi}_j + \tilde{r}_j, \quad \dot{\tilde{r}}_j = -k_{r_j}\tilde{r}_j. \tag{16}$$

Hence, the controller (13) guarantees that for all initial conditions $\tilde{\psi}(t_0), \tilde{r}(t_0) \in \mathbb{R}\times\mathbb{R}$, $t_0 \in \mathbb{R}^+$, the vehicle tracks the LOS angle $\psi_{\text{LOS},j}$, as given by (12), and the LOS angle rate $\dot{\psi}_{\text{LOS},j}$.

To show that the proposed LOS controller achieves the path following control goals (7), (8), we first define the path following error for vehicle j as $e_j \triangleq y_j - D_{y_j}$. Differentiating e_j with respect to time and using (2) and (12) we obtain

$$\dot{e}_j = -u_{c_j}(t)\frac{e_j}{\sqrt{e_j^2+\Delta^2}} + v_j\frac{\Delta}{\sqrt{e_j^2+\Delta^2}} + \boldsymbol{h}_j^T \begin{bmatrix} \tilde{u}_j \\ \tilde{\psi}_j \end{bmatrix}. \tag{17}$$

where $\boldsymbol{h}_j^T = [h_{1,j}(\tilde{\psi}, \psi_{\text{LOS}}) \;\; h_{2,j}(t, \tilde{\psi}, \psi_{\text{LOS}}, v_j)]$ and

$$\begin{aligned} h_{1,j} &= \sin(\tilde{\psi}_j + \psi_{\text{LOS},j}) \\ h_{2,j} &= [u_{c_j}(t)(\sin(\tilde{\psi}_j + \psi_{\text{LOS},j}) - \sin\psi_{\text{LOS},j}) \\ &\quad + v_j(\cos(\tilde{\psi}_j + \psi_{\text{LOS},j}) - \cos\psi_{\text{LOS},j})]/\tilde{\psi}_j. \end{aligned}$$

System (17) can be seen as a nominal system perturbed by the expoentially converging surge speed tracking error $\tilde{u}_j$ and the yaw angle tracking error $\tilde{\psi}_j$. In particular, system (17) interconnected with (15) and (16) is a cascaded system. Moreover, under the assumptions (5), (6) the nominal path following error system, i.e. system (17) with $\tilde{u}_j = \tilde{\psi}_j = 0$, is uniformly globally asymptotically stable (UGAS) and uniformly locally exponentially stable (ULES). This can be proven using the quadratic Lyapunov function $V = 1/2e_j^2$ (see [8]). Furthermore, the perturbing inputs $\tilde{u}_j$ and $\tilde{\psi}_j$ are exponentially vanishing, as systems (15) and (16) are UGES. Then by application of [9] (Theorem 7 and Lemma 8) the cascade of system (17) with (15) and (16) is UGAS and ULES (see [8]). This implies that the cross-track error $e_j \to 0$ exponentially, in any ball of initial conditions, and hence the cross-track control goal (7) is achieved exponentially. Subsequently, this implies that $\psi_{\text{LOS,j}} \to 0$ exponentially (see Eq. (12)). Since ψ_j tracks $\psi_{\text{LOS,j}}$ exponentially, we conclude that the orientation control goal (8) is achieved exponentially, in any ball of initial conditions. □

The requirement imposed in Proposition 1 that the commanded velocity u_{c_j} is separated from zero, i.e. that $u_{c_j}(t) > U_{\min}$, $\forall t \geq t_0$, comes from the underactuation of the vehicles. In particular, the vehicles are uncontrollable at zero velocity and $u_{c_j} = 0$ would prevent the achievement of the path following control goals (7), (8). Moreover, the requirement that $u_{c_j}(t) < U_{\max}$, $\forall t \geq t_0$, where $U_{\max} < \Delta/C_v$, is needed to ensure stability of the cross-track error. Essentially, the condition on $U_{\max}$ says that the look-ahead distance must be chosen in accordance with the maximum permissible speed, which is natural for any LOS-based design.

An important implication of Proposition 1 is that the resulting dynamics in the x-direction is given by

$$\dot{x}_j = u_{c_j}(t) + \boldsymbol{\pi}_j^T\boldsymbol{\chi}_j, \;\; j = 1, \ldots, n, \tag{18}$$

where $\boldsymbol{\chi}_j \triangleq [\tilde{u}_j, \psi_j]^T$ decays to zero exponentially if the conditions of Proposition 1 are satisfied. In particular, it is required that $u_{c_j} \in (U_{\min}, U_{\max})$, $\forall t \geq t_0$, which is guaranteed by a proper choice of control law for u_{c_j}. This statement is made more clear in Section IV. The interconnection term $\boldsymbol{\pi}_j = [\pi_{1,j}(\psi_j), \pi_{2,j}(t, \psi_j, v_j)]^T$ in (18) is given by

$$\pi_{1,j} = \cos(\psi_j), \qquad \pi_{2,j} = u_{c_j}(t)\frac{\cos\psi_j - 1}{\psi_j} - v_j\frac{\sin\psi_j}{\psi_j}.$$

Note that the functions $\pi_{i,j}$, $i = 1, 2$, are globally bounded as $|\sin x/x| \leq 1$, $|(\cos x - 1)/x| < 1$, $\forall x \in \mathbb{R}$, and $u_{c_j}(t) < U_{\max}$, $|v_j(t)| < U_{\max}$, $\forall t \geq t_0$.

IV. Nonlinear Coordination

Under control (11) and (13), control goals (7) and (8) are achieved exponentially provided that the commanded speeds for all vehicles satisfy the controllability constraint $u_{c_j}(t) \in (U_{\min}, U_{\max})$, $\forall t \geq t_0$, $j = 1, \ldots, n$, cf. Proposition 1. Moreover, after transients, the remaining dynamics in the x-direction track the commanded velocity profile $u_{c_j}(t)$, $j = 1, \ldots, n$, as given by (18).

In order to satisfy the remaining control goal (9), the vehicles have to adjust their forward speeds to coordinate their motion with each other so as to achieve the desired formation pattern and move with the desired velocity profile $u_d(t)$. The dynamics in the x direction, given by (18), suggests that this can be achieved by designing appropriate coordination controllers for u_{c_j}, $j = 1, \ldots, n$. Such controllers must also satisfy the controllability constraint $u_{c_j}(t) \in (U_{\min}, U_{\max})$ so as not to interfere with the achievement of the path following control goals, cf. Proposition 1. Moreover, the coordination controllers must respect topological and directional limitations of the communication network, i.e. that all-to-all communication may not be available and that some, or all, of the communication links may be unidirectional.

To describe the communication between the n vehicles in the formation, we use a directed graph $\mathcal{G}(\mathcal{V}, \mathcal{E})$, where the set $\mathcal{V}(\mathcal{G})$ is called the vertex set of $\mathcal{G}$ and the set $\mathcal{E}(\mathcal{G})$ is called the edge set of $\mathcal{G}$. The elements of $\mathcal{V}(\mathcal{G})$ are called vertices and vertex j corresponds to vehicle j in the formation. The elements of $\mathcal{E}(\mathcal{G})$ are called edges, and the edge set consists of ordered pairs of distinct vertices of $\mathcal{G}$. For our purposes, it is convenient to use the following convention: if vehicle i transmits information to vehicle j, then there is an edge *from* node j *to* node i, i.e. $(j, i) \in \mathcal{E}(\mathcal{G})$. That is, the edge is in the opposite direction of the information flow, see Figure 4. Moreover, we denote by $\mathcal{A}_j$ the set of all nodes

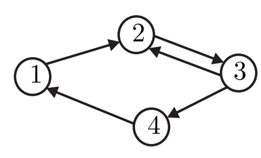

Fig. 4. Communication graph.

i such that there is an edge from node j to node i (i.e. $\mathcal{A}_j$ consists of all vehicles i transmitting information to vehicle j). Furthermore, if there is a path in the graph from node i to node j, then j is said to be reachable from i. Node j is *globally* reachable if it is reachable from every other node in the graph.

Before proceeding, we make the following natural assumption on the desired velocity $u_d(t)$: there exists $a > 0$ such that

$$u_d(t) \in [U_{\min} + a, U_{\max} - a], \quad \forall t \geq t_0. \tag{19}$$

To solve the coordination problem, we propose the following control law for u_{cj}, $j = 1, \ldots, n$:

$$u_{cj} = u_d(t) - g\left(\sum_{i \in \mathcal{A}_j} (x_j - x_i - d_{ji})\right), \tag{20}$$

Here $d_{ji} \triangleq D_{x_j} - D_{x_i}$ corresponds to the desired distance along the x-axis between the jth and ith vehicle in the group. The function $g(x)$ is continuously differentiable, satisfying $g'(0) > 0$, $g(0) = 0$ and $g(x) \in (-a, a)$, where a is the parameter defined in (19). The function g can be chosen, for example, equal to $g(x) \triangleq 2a/\pi \tan^{-1}(x)$.

Under these assumptions on g and under the assumption that the desired speed profile $u_d(t)$ satisfies (19), the proposed u_{c_j} given by (20) lie within the set $(U_{\min}, U_{\max})$ for all values of its arguments. Notice that linear coordination control laws without the nonlinearity g, which are used for example in [1] and [3], are not applicable in our case since they inevitably violate the controllability constraint $u_{c_j}(t) \in (U_{\min}, U_{\max})$. The proposed coordination controller satisfies the communication constraints given by the graph $\mathcal{G}$, in the sense that the commanded speed u_{cj} for the jth vehicle depends only on the variables x_i of the vehicles transmitting information to the jth vehicle.

The properties of the proposed coordination controllers are summarized in the following proposition.

Proposition 2. *Suppose $u_d(t)$ satisfies (19) with $U_{\min} > 0$ and $U_{\max} < \Delta/C_v$ and the communication graph $\mathcal{G}$ has at least one globally reachable node. Then n vehicles described by (1)-(4) in closed loop with controllers (11), (13) and (20) achieve control goals (7)-(9) exponentially.*

Prior to proving Proposition 2, let us formulate a technical result on a network of scalar systems

$$\dot{\theta}_j = -\sum_{i \in \mathcal{A}_j} \lambda_{ji}(\boldsymbol{\theta})(\theta_j - \theta_i), \qquad j = 1, \ldots, n, \tag{21}$$

with an underlying communication graph $\mathcal{G}$, where $\boldsymbol{\theta} \triangleq [\theta_1, \ldots, \theta_n]^T$ and $\lambda_{ji}(\boldsymbol{\theta}) > 0$ are some scalar functions. Denote $\mathbb{1} \triangleq [1, \ldots, 1]^T$.

Lemma 1. *Consider system (21). If $\mathcal{G}$ has a globally reachable node, then the dynamics of $\boldsymbol{\delta} \triangleq \boldsymbol{\theta} - \left(\frac{1}{n}\sum_{i=1}^n \theta_i\right)\mathbb{1}$ are GAS at the origin.*

Proof. It is shown in [10] Theorem 3 that under the conditions of the Lemma, system (21) is global asymptotic stability (GAS) with respect to the set $\Omega = \{\boldsymbol{\theta} : \boldsymbol{\theta} = \alpha\mathbb{1}, \alpha \in \mathbb{R}\}$. Notice that $\boldsymbol{\theta}$ is decomposed into the sum of $\left(\frac{1}{n}\sum_{i=1}^n \theta_i\right)\mathbb{1} \in \Omega$ and $\boldsymbol{\delta}$, which is orthogonal to the elements of Ω (since $\boldsymbol{\delta}^T\mathbb{1} = 0$). Therefore, GAS of the set Ω for system (21) is equivalent to the fact that the dynamics of $\boldsymbol{\delta}$ are GAS at the origin. □

Sketch of proof of Proposition 2. By assumption $u_d(t)$ satisfies (19) with $U_{\min} > 0$ and $U_{\max} < \Delta/C_v$, and the coordination control law (20) guarantees that the commanded velocity for vehicle j satisfies $u_{c_j}(t) \in (U_{\min}, U_{\max})$. Then, for a marine vehicle (1)-(4), satisfying assumptions (5) and (6), all the assumptions of Proposition 1 are satisfied and it follows that the control goals (7) and (8) are achieved exponentially.

Furthermore, under Proposition 1, the resulting dynamics of the vehicles in the x-direction are given by (18). Inserting the commanded velocity profile (20), the dynamics of (18) are given by

$$\dot{x}_j = u_d(t) - g\left(\sum_{i \in \mathcal{A}_j} (x_j - x_i - d_{ji})\right) + \boldsymbol{\pi}_j^T \boldsymbol{\chi}_j. \tag{22}$$

From the coordination control goal (9), we define the coordination variable for vehicle j as $\theta_j \triangleq x_j - D_{x_j} - \int_{t_0}^t u_d(\sigma)d\sigma$, $j = 1, \ldots, n$. Deriving the θ_j-dynamics and using (22) we obtain

$$\dot{\theta}_j = -g\left(\sum_{i \in \mathcal{A}_j} (\theta_j - \theta_i)\right) + \boldsymbol{\pi}_j^T \boldsymbol{\chi}_j. \tag{23}$$

Notice that the term $\boldsymbol{\pi}_j^T \boldsymbol{\chi}_j$ depending on the states of the j'th vehicle exponentially decays along solutions of the closed-loop system since $\boldsymbol{\pi}_j$ is globally bounded and $\boldsymbol{\chi}_j$ is an exponentially decaying term (see Section III).

Define the average position of the vehicles as $\alpha \triangleq \frac{1}{n}\sum_{i=1}^n \theta_i$ and the distances from the vehicles to α as $\delta_j \triangleq \theta_j - \alpha$, $j = 1, \ldots, n$. Using the vector notation, we have $\boldsymbol{\delta} = \boldsymbol{\theta} - \alpha\mathbb{1}$. We will show that $\boldsymbol{\delta}(t)$ exponentially decays to zero and $\alpha(t) \to \alpha_0$, as $t \to \infty$, exponentially, where α_0 is some constant. Notice that this implies that $\theta_j(t) \to \alpha_0$, as $t \to \infty$, for all $j = 1, \ldots, n$. In turn, this yields the achievement of control goal (9) in the original coordinates x_j, $j = 1, \ldots, n$.

Let us first derive the dynamics of α and $\boldsymbol{\delta}$. Using (23) and taking into account the definition of α and the fact that $\theta_j - \theta_i = \delta_j - \delta_i$, we obtain

$$\dot{\alpha} = f(\boldsymbol{\delta}) + \epsilon_\alpha(t) \tag{24}$$

where $f(\boldsymbol{\delta}) \triangleq -\frac{1}{n}\sum_{j=1}^n g\left(\sum_{i \in \mathcal{A}_j}(\delta_j - \delta_i)\right)$ and $\epsilon_\alpha = \frac{1}{n}\sum_{j=1}^n \boldsymbol{\pi}_j^T \boldsymbol{\chi}_j$. From (23) and the definition of $\boldsymbol{\delta}$, we obtain

$$\dot{\boldsymbol{\delta}} = \boldsymbol{F}(\boldsymbol{\delta}) + \boldsymbol{\epsilon}_\delta(t), \tag{25}$$

where $F_j(\boldsymbol{\delta}) \triangleq -g\left(\sum_{i \in \mathcal{A}_j}(\delta_j - \delta_i)\right) - f(\boldsymbol{\delta})$ and $\epsilon_{\delta_j} \triangleq \boldsymbol{\pi}_j^T \boldsymbol{\chi}_i - \epsilon_\alpha$, $j = 1, \ldots, n$.

Let us first show that system

$$\dot{\boldsymbol{\delta}} = \boldsymbol{F}(\boldsymbol{\delta}), \tag{26}$$

is GAS at the origin. Consider system (23) with $\boldsymbol{\pi}_j^T \boldsymbol{\chi}_j = 0$. Applying the mean value theorem to the right-hand side of

(23), we obtain

$$\dot{\theta}_j = -g'(\psi_j(\boldsymbol{\theta})) \sum_{i \in \mathcal{A}_j} (\theta_j - \theta_i) \triangleq - \sum_{i \in \mathcal{A}_j} \lambda_{ji}(\boldsymbol{\theta})(\theta_j - \theta_i), \tag{27}$$

where $\lambda_{ji}(\boldsymbol{\theta}) = g'(\psi_j(\boldsymbol{\theta}))$ and $\psi_j(\boldsymbol{\theta})$ is a point lying on the line segment $[0, \sum_{i \in \mathcal{A}_j}(\theta_j - \theta_i)]$. Since $g'(x) > 0$ for all $x \in \mathbb{R}$, we have $\lambda_{ji}(\boldsymbol{\theta}) > 0$ for all $\boldsymbol{\theta} \in \mathbb{R}^n$. Applying Lemma 1 we conclude that the dynamics of $\boldsymbol{\delta}$, which coincides with (26), is GAS at the origin.

To show that all solutions of (25) with the exponentially decayig term $\boldsymbol{\epsilon}_\delta(t)$ converge to zero we only need to show that the solutions of (25) remain bounded (see [11] on Converging Input Converging State (CICS) property). Boundedness of $\boldsymbol{\delta}(t)$ can be proven using the Lyapunov function $V(\boldsymbol{\delta}) = \max_i \delta_i - \min_i \delta_i$. This function is positive definite, since by definition of $\boldsymbol{\delta}$ we have $\boldsymbol{\delta}^T \mathbb{1} = \sum_{i=1}^n \delta_i = 0$. This implies that $\max_i \delta_i \geq 0$ and $\min_i \delta_i \leq 0$. Therefore, $V(\boldsymbol{\delta})$ is positive definite and radially unbounded since $||\boldsymbol{\delta}|| \to +\infty$ implies $V(\boldsymbol{\delta}) \to +\infty$. It can be shown that the derivative[1] of $V(\boldsymbol{\delta})$ along the solutions of (25) satisfies

$$\dot{V}(\boldsymbol{\delta}) \leq 2 \max_j |\epsilon_{\delta_j}(t)|. \tag{28}$$

Moreover, since $\boldsymbol{\epsilon}_\delta(t)$ is an exponentially decaying term, we obtain

$$\dot{V}(\boldsymbol{\delta}) \leq C e^{-at}, \tag{29}$$

for some $C > 0$, $a > 0$. Integrating the last inequality, we obtain

$$V(\boldsymbol{\delta}(t)) \leq V(\boldsymbol{\delta}(t_0)) + \text{Const}. \tag{30}$$

Hence, $V(\boldsymbol{\delta}(t))$ is bounded for $t \geq t_0$, which implies boundedness of $\boldsymbol{\delta}(t)$. Applying Theorem 1 from [11], we conclude that every solution of (25) converges to zero. Moreover, it can be shown that the linearization of (26) is exponentially stable at the origin. This, in turn, implies that the right-hand side of (24) exponentially converges to zero. By integrating (24) we conclude that $\alpha(t) \to \alpha_0$ as $t \to \infty$, for some $\alpha_0 \in \mathbb{R}$, and the convergence is exponential. This concludes the proof of the Proposition. □

V. Simulations

The proposed formation control scheme has been implemented in Simulink™ and simulated for the case of three surface vessels. The desired straight line paths and desired inter-vehicle spacing is given by $(D_{x1}, D_{y1}) = (-100, 50)$, $(D_{x2}, D_{y2}) = (0, 0)$, $(D_{x3}, D_{y3}) = (-100, -50)$, see Section II-B. The desired velocity profile $u_d(t)$ is chosen as $u_d = 5.0$ m/s. The controller gains are chosen as $k_u = 0.5$ and $k_\psi = 0.5$, $k_r = 5$ and $\Delta = 70$ respectively. The function $g(x)$ is chosen as $g(x) = \frac{2}{\pi} \tan^{-1}(x) \in (-1, 1)$ and the communication topology is shown in Figure 5.

The simulation results are shown in Fig. 6(a)-6(d) and the presented simulation results clearly show that the control goals (7)-(9) are achieved.

[1] Since $V(\boldsymbol{\delta})$ is only continuous and locally Lipschitz, by $\dot{V}(\boldsymbol{\delta})$ we mean the Dini derivative, see [10].

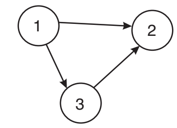

Fig. 5. Example: communication graph.

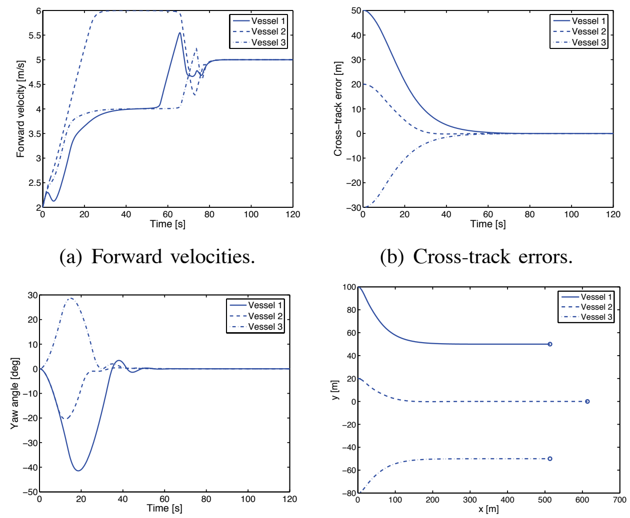

(a) Forward velocities. (b) Cross-track errors.

(c) Yaw angles. (d) xy-trajectories.

Fig. 6. Example: simulation results.

References

[1] R. Skjetne, S. Moi, and T. I. Fossen, "Nonlinear formation control of marine craft," in *Proc. 41st IEEE Conference on Decision and Control*, Las Vegas, NV, USA, Dec 2002, pp. 1699–1704.

[2] L. Lapierre, D. Soetanto, and A. Pascoal, "Coordinated motion control of marine robots," in *Proc. 6th IFAC Conference on Manoevering and Control of Marine Craft*, Girona, Spain, 2003.

[3] R. Ghabcheloo, A. Pascoal, C. Silvestre, and D. Carvalho, "Coordinated motion control of multiple autonomous underwater vehicles," in *Proc. International Workshop on Underwater Robotics*, Genoa, Italy, Nov 2005, pp. 41–50.

[4] A. P. Aguiar, R. Ghabcheloo, A. Pascoal, C. Silvestre, J. Hespanha, and I. Kaminer, "Coordinated path-following of multiple underactuated autonomous vehicles with bidirectional communication constraints," in *Proc. International Symposium on Communications, Control and Signal Processing*, Morocco, March 2006.

[5] E. Børhaug, A. Pavlov, and K. Y. Pettersen, "Cross-track formation control of underactuated autonomous underwater vehicles," in *Group Coordination and Cooperative Control*, K. Y. Pettersen, J. T. Gravdahl, and H. Nijmeijer, Eds. Springer Verlag, 2006, vol. 336.

[6] T. I. Fossen, *Marine Control Systems*. Trondheim, Norway: Marine Cybernetics, 2002.

[7] E. Fredriksen and K. Pettersen, "Global κ-exponential way-point manoeuvering of ships," in *Proc. 43rd IEEE Conference on Decision and Control*, Bahamas, Dec 2004, pp. 5360–5367.

[8] E. Børhaug, A. Pavlov, and K. Y. Pettersen, "Cross-track formation control of underactuated surface vessels," in *Proc. 45th IEEE Conference on Decision and Control*, San Diego, CA, USA, Dec 2006.

[9] E. Panteley, E. Lefeber, A. Loria, and H. Nijmeijer, "Exponential tracking control of mobile car using a cascaded approach," in *Proc. IFAC Workshop on Motion Control*, Grenoble, France, 1998, pp. 221–226.

[10] Z. Lin, B. Francis, and M. Maggiore, "On the state agreement problem for multiple nonlinear dynamical systems," in *16th IFAC World Congress*, 2005.

[11] E. Sontag, "A remark on the converging-input converging-state property," *IEEE Trans. Automatic Control*, vol. 48, no. 2, pp. 313–314, 2003.